JOURNAL OF PROPULSION AND POWER
Vol. 21, No. 4, July–August 2005

Hybrid Neural-Network Genetic-Algorithm Technique for Aircraft Engine Performance Diagnostics

Takahisa Kobayashi*
QSS Group, Inc., Cleveland, Ohio 44135
and
Donald L. Simon†
U.S. Army Research Laboratory, NASA John H. Glenn Research Center at Lewis Field, Cleveland, Ohio 44135

In this paper, a model-based diagnostic method, which utilizes neural networks and genetic algorithms, is investigated. Neural networks are applied to estimate the engine internal health, and genetic algorithms are applied for sensor bias detection and estimation. This hybrid approach takes advantage of the nonlinear estimation capability provided by neural networks while improving the robustness to measurement uncertainty through the application of genetic algorithms. The hybrid diagnostic technique also has the ability to rank multiple potential solutions for a given set of anomalous sensor measurements in order to reduce false alarms and missed detections. The performance of the hybrid diagnostic technique is evaluated through some case studies derived from a turbofan engine simulation. The results show that this approach is promising for reliable diagnostics of aircraft gas turbine engines.

Introduction

OVER the last several decades, significant research efforts have been directed at the development of performance diagnostic systems for aircraft gas turbine engines. Such systems can provide a variety of benefits to aircraft operators including improved safety,[1] improved reliability, and reduced operating costs. With the significant growth in air traffic projected in the coming years, it is expected that the demand for enhanced diagnostic methods will continue to increase.

Aircraft engine performance diagnostics is, in general, accomplished by accurately estimating a set of engine component performance parameters, or health parameters, from available sensor measurements.[2–4] Health parameters, such as efficiency and flow capacity of engine components, indicate the level of component performance deterioration. They deviate from the nominal baseline gradually with time as a result of normal usage and also abruptly as a result of anomalous events such as foreign object damage. The sensor measurements, which include gas path temperatures and pressures, spool speeds, fuel flows, and variable geometry, provide information regarding the health of the engine. The general approach to performance diagnostics can be expressed using the following relationship between the engine health parameters and the sensed parameters:

$$\boldsymbol{y} = f(\boldsymbol{p}, \text{operating condition}) + \boldsymbol{w} \tag{1}$$

where $\boldsymbol{y}$ and $\boldsymbol{p}$ represent the vectors of sensed parameters and engine health parameter deltas (deviations from the nominal), respectively. The closed-loop engine behavior is represented by $f(\cdot)$, which is a nonlinear function of $\boldsymbol{p}$ and operating condition such as altitude, Mach number, and engine power level. The vector $\boldsymbol{w}$ represents measurement inaccuracies including bias and white noise. The problem is to estimate the health parameter vector $\boldsymbol{p}$ given the sensed parameter vector $\boldsymbol{y}$. The length of time available to solve this problem depends on the application objectives (e.g., real-time in-flight fault detection, postflight ground-based trend monitoring).

Several issues make this problem highly challenging. First, the only information available for health parameter estimation is the sensed parameters, and the number of health parameters to be estimated is often greater than the number of sensors available. For such an underdetermined problem, there exist an infinite number of solutions for a given set of sensor measurements, and some assumptions must be made to select the best or most probable solution. One option for trend monitoring purposes is to assume that the most likely solution has the minimum deviation from the condition estimated in the previous time frame assuming the health condition is expected to degrade gradually rather than rapidly.

A second issue is that accurate estimation of health parameters might not be achieved if sensor locations are not appropriate. For instance, assume that a health parameter is primarily affecting the flow condition in the bypass duct and has a minor influence on the core flow. It will be difficult to estimate this health parameter from core measurements alone even if there are an excessive number of sensors. In such a case, some heath parameters are unobservable because critical measurements are missing.

Another challenging issue is that sensor noise and bias distort the sensor measurements as described in Eq. (1), thereby masking the true condition of the engine and leading to incorrect estimation results. Accurate statistical information to characterize measurement uncertainty is often not available, and filtering techniques are ineffective against biases. Because of their time-invariant characteristic, sensor biases can be treated as unknown parameters to be estimated in addition to the health parameters. However, this obviously increases the number of unknowns in the estimation problem.

Finally, the combined effect of system nonlinearity and sensor selection can result in multiple health deterioration scenarios producing similar measurement shifts. This is a difficult problem to deal with because estimation techniques, in general, give only one set of estimated health parameters for a given set of measurements without the capability to indicate the level of confidence in the results. One possible approach that addresses this issue involves the use of a failure database developed a priori from flight tests or simulation; several possible solutions are selected from the database, and a confidence level is determined using statistical approaches. Incorporation of intelligent logic in the diagnostic system architecture is indispensable in determining the most reasonable solution in

Presented as Paper 2001-3763 at the AIAA/ASME/SAE/ASEE 37th Joint Propulsion Conference and Exhibit, Salt Lake City, UT, 8–11 July 2001; received 7 April 2004; revision received 7 December 2004; accepted for publication 9 December 2004.

*Aerospace Engineer.
†Electronics Engineer.

the highly nonlinear and noise-corrupted problem environment. A performance diagnostic system without the capability to deal with these issues will exhibit unacceptable false alarm or missed detection rates.

Researchers have investigated a number of estimation techniques such as weighted least-squares,[4,5] Kalman filters,[3,6,7] neural networks,[8] and genetic algorithms.[9,10] Some of these techniques were applied for real-time in-flight diagnostics while some were applied for ground-based diagnostics. Each approach has relative strengths; however, a technique that is capable of addressing all of the preceding issues has not yet emerged. In this paper, a diagnostic technique is investigated for ground-based steady-state trend monitoring of aircraft gas turbine engines. The objective of the steady-state trend monitoring is to estimate health parameters accurately from sensor outputs collected at steady-state conditions. Steady state is defined as the condition where transient behavior induced by the power-lever-angle movement has been dissipated. It is assumed that at most one sensor can be biased at a time. This diagnostics problem is approached through a model-based diagnostic method utilizing neural networks and genetic algorithms. The proposed technique takes advantage of the nonlinear estimation capability provided by neural networks while improving the robustness to measurement uncertainty caused by bias through the application of genetic algorithms. The hybrid diagnostic technique also has the capability to rank multiple potential solutions for a given set of anomalous sensor measurements in order to reduce false alarms and missed detections.

Model-Based Diagnostics

One approach to aircraft engine performance diagnostics that has been investigated by a number of researchers is called model-based diagnostics (MBD). As shown in Fig. 1, the MBD architecture is composed of an engine model and an associated parameter estimation algorithm for monitoring engine component performance deterioration. The engine model can be a linear or nonlinear representation of the physical engine. As the physical engine is operated over a length of time, its component performance degrades from the nominal level, and consequently the sensor output values deviate from their nominal condition values. In the MBD architecture, the health parameter estimates $\hat{\boldsymbol{p}}$ are computed based on the difference between the engine model outputs and the physical engine sensor outputs. Accurately estimated health parameters result in good agreement between the engine model outputs and the physical engine sensor outputs, while indicating the level of component performance deterioration that the physical engine is experiencing.

Accurately estimated health parameters and a "tuned" engine model can provide a variety of benefits. Health parameter estimates can be used to determine when maintenance actions need to be taken. A tuned engine model, which represents the physical engine at a degraded condition, can be implemented onboard, depending on its complexity, within the digital engine control unit and used to achieve safety benefits during flight. The tuned engine model provides estimated sensor outputs as well as estimates of unmeasurable parameters such as thrust and compressor stall margins. With these estimated parameters, a variety of accommodating actions can be performed to prevent the progression of damage.

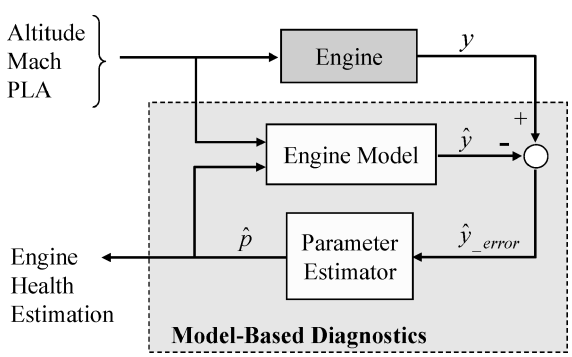

Fig. 1 Model-based diagnostics architecture.

The MBD system presented in this paper utilizes a nonlinear engine model and a hybrid parameter estimation technique based on neural networks and genetic algorithms. In the following sections, these two main parts of the MBD system are discussed in detail.

Engine Model

The engine model used in this paper is a nonlinear simulation of an advanced military twin-spool turbofan engine. This engine model has been constructed as a component-level model (CLM),[11] which assembles the major components of an aircraft engine. The CLM represents highly complex engine physics while having the capability to run in real time. Engine performance deterioration is modeled by adjustments to efficiency and/or flow coefficient scalars of the following components: fan (FAN), booster (BST), high-pressure compressor (HPC), high-pressure turbine (HPT), and low-pressure turbine (LPT). A set of nine health parameters must be estimated accurately in order to diagnose the engine health condition: 1, FAN efficiency; 2, FAN flow; 3, BST flow; 4, HPC efficiency; 5, HPC flow; 6, HPT efficiency; 7, HPT flow; 8, LPT efficiency; and 9, LPT flow. There are 17 engine outputs and three actuator outputs that can potentially be measured by sensors. In a realistic application, such a large set of sensors would not be available. After some investigation, a set of 12 sensed parameters was selected: 1, N2 (low-pressure spool speed); 2, N25 (high-pressure spool speed); 3, T27 (HPC inlet temperature); 4, T3 (combustor inlet temperature); 5, PS15 (bypass duct static pressure); 6, PS21 (fan exit static pressure); 7, P27D (booster tip pressure); 8, PS3 (combustor inlet static pressure); 9, P42 (interturbine pressure); 10, WF36 (fuel flow); 11, A8 (nozzle area); and 12, A16 (variable bypass duct area). In the current study, the performance of the MBD system is evaluated in the simulation environment. The engine model is used to represent both the physical engine and the MBD system engine model.

Sensor Measurement Inaccuracy

The sensor output data collected during flight usually contain a significant amount of noise. In the steady-state trend monitoring problem, the amount of noise can be reduced by averaging sensor output values over some time interval. If data are collected at the frequency of 50 Hz, then a 1-s steady-state operation provides 50 samples to be averaged. This averaging, however, does not completely remove sensor output inaccuracy. The noise model used in this paper represents steady-state noise, that is, sensor output inaccuracy after the averaging of samples. It can be considered as small biases that existed during the data sampling at a particular time. This steady-state noise is assumed to be zero-mean, normally distributed white noise. Its standard deviation was derived from available data, and its magnitude is much smaller than the noise level observed in raw data. From this point on, the word "noise" means steady-state noise.

Nonuniqueness of Health Degradation Effects on Sensor Outputs

One of the challenges often encountered in the health estimation problem is that the effects of health degradation on sensor outputs are not unique. Specifically, there is a chance that distinct health degradation cases will result in indistinguishable shifts in sensor measurements.[2] As discussed earlier, this nonuniqueness can be the result of the combined effect of system nonlinearity and sensor selection. Such a phenomenon can be observed in the highly nonlinear military engine model used in this paper. An example is shown in Fig. 2, which compares the measurement shifts for two health degradation scenarios at cruise condition: case A for 2% degradation in FAN and LPT efficiencies and case B for a 3% degradation in FAN efficiency. The two cases are distinct; however, the differences in all sensor measurements between these two cases are within the range of noise. This means that, in the health parameter estimation problem, multiple solutions exist for a given set of measurement shifts.

One option that might be able to address this issue is to incorporate some intelligent logic that can provide a list of possible degradation scenarios for a given set of measurement shifts, as demonstrated

in Ref. 12. Even if a diagnostic system cannot give a definitive answer, such a list can provide very useful information to maintenance personnel attempting to troubleshoot anomalous engine behavior. Another option is to use sensor measurements from more than one operating point so that a unique set of measurement shifts can be assigned for each degradation scenario. This approach takes advantage of the nonlinearity of the system behavior at different operating points. Diagnostics based on multiple operating points[10,13] has been investigated by several researchers, but it has some limitations. First, it must be assumed that a given health degradation does not progress as multiple operating points are traversed. Second, increasing the number of measurements also increases the chance of uncertain factors entering to the available measurements at hand. For instance, different sensors can be biased at different operating points. Third, in the case of steady-state trend monitoring the engine is required to reach steady-state conditions at multiple operating points. As the number of operating points increases, the impact of the preceding three issues increases, and a multipoint diagnostic approach becomes less practical.

Hybrid Neural-Network Genetic-Algorithm Estimation Architecture

Accurately estimating the health parameters is a critical issue for the development of an MBD system. Any estimation architecture must be able to handle nonlinearity as well as be robust to sensor noise and bias as discussed earlier. The estimation architecture in this paper combines neural networks and genetic algorithms (GA) for aircraft engine performance diagnostics based on the steady-state flight data. The objective is to estimate health parameters accurately from sensor outputs collected at steady-state conditions even in the presence of a biased measurement. Similar to Refs. 3 and 4, it is assumed that at most one sensor can be biased at a time to make the problem manageable. Neural networks exhibit excellent nonlinear estimation capabilities, but the training set required to fully represent all possible permutations of health parameters and sensor bias is prohibitively large. It would take excessive time to train such neural networks, and their performance might not reach a satisfactory level. To avoid this problem, the approach taken by the hybrid estimator designates neural networks for the health estimation task while designating GA for the sensor bias detection task. This approach reduces the size of the training set significantly.

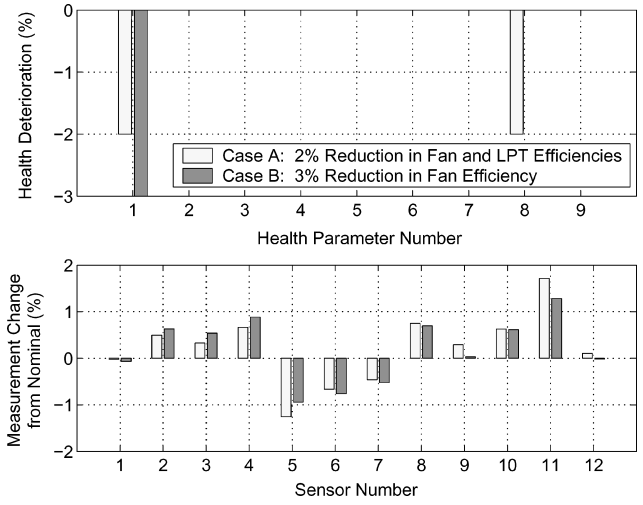

Fig. 2 Comparison of two degradation cases at cruise condition.

The problem setup is shown in Fig. 3. The vector $\boldsymbol{p}$ represents a set of health parameter deltas to be estimated. In the simulation environment, the measurement uncertainty vector in Eq. (1) is decomposed as

$$\boldsymbol{w} = \boldsymbol{b} + \boldsymbol{v} \tag{2}$$

where $\boldsymbol{b}$ and $\boldsymbol{v}$ represent a bias vector and a steady-state white-noise vector, respectively. Because it is assumed that one sensor can be biased at a time, the bias vector contains one nonzero value at most, and its magnitude is large relative to the expected noise level. This vector will be estimated; however, the estimated value of the nonzero element will be under the influence of noise to some degree because bias and noise contained in measurements are indistinguishable. Therefore, an estimated bias vector will have only one nonzero value, just as the actual bias vector $\boldsymbol{b}$ does, but the estimated value will be an approximation of the combined value of bias and noise contained in the uncertainty vector $\boldsymbol{w}$. The unknown vectors $\boldsymbol{p}$ and $\boldsymbol{b}$ must be estimated based on the available physical sensor measurements $\boldsymbol{y}$.

As shown in the figure, the hybrid estimator is composed of the bias data set, the neural-network estimator, and the GA optimization technique. The bias data set, which is composed of a large number of bias vectors, is defined a priori and is used by the GA in the search for a bias vector that matches well with an actual bias contained in the measurement vector. The neural-network estimator is trained off-line with noise-corrupted but bias-free sensor measurements. It will perform sufficiently well in estimating health parameters as long as the sensor measurements do not contain any bias. For a given set of estimated health parameters and sensor bias, the engine model is executed, and its outputs are evaluated against the physical sensor measurements. The bias data set, the neural-network estimator, and the engine model are coordinated by the GA in the search for an optimal solution.

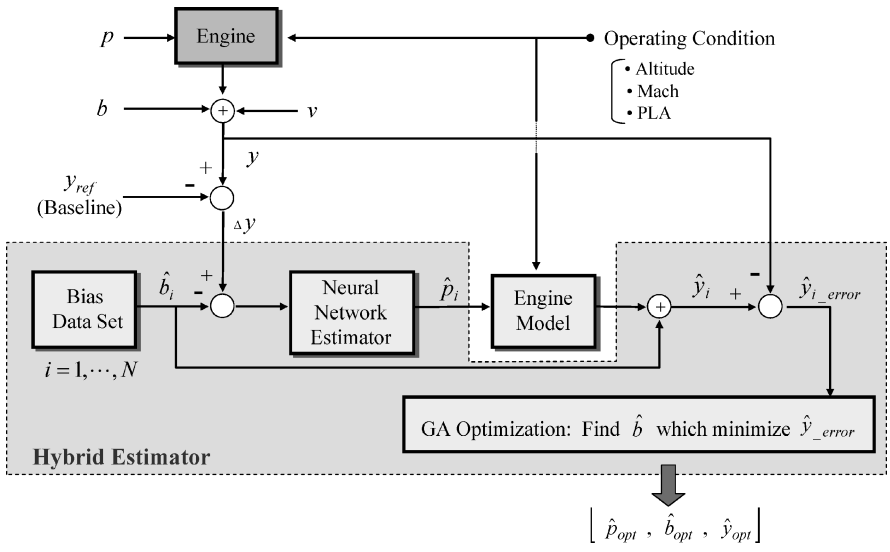

Fig. 3 Hybrid engine health estimation architecture.

Table 1 Performance comparison of neural-network estimators

	Single-point design at cruise		Two-point design at cruise and takeoff	
Health parameter	Mean absolute error, %	Standard deviation of % error	Mean absolute error, %	Standard deviation of % error
FAN efficiency	9.00	13.01	5.55	9.15
FAN flow	5.42	9.28	2.92	4.77
BST flow	6.08	9.90	5.03	8.55
HPC efficiency	9.64	15.22	4.19	7.79
HPC flow	9.39	15.69	5.52	9.30
HPT efficiency	8.86	14.66	4.91	8.50
HPT flow	2.94	4.92	1.51	2.65
LPT efficiency	10.33	15.16	6.38	10.09
LPT flow	5.63	9.11	2.79	4.70

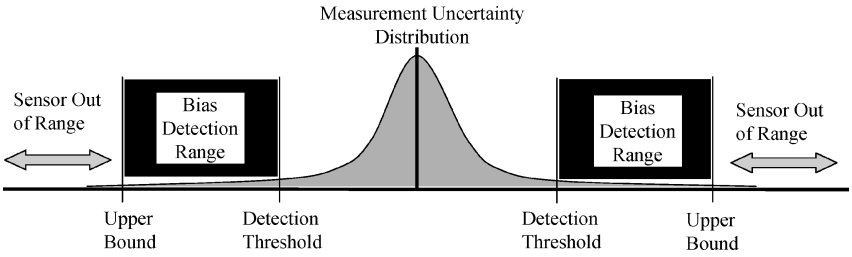

Fig. 4 Measurement uncertainty distribution with bias detection threshold.

Bias Data Set

The bias data set defines the solution space over which the GA searches for an optimal sensor bias solution that will cancel out the actual bias in the measurements. It is composed of bias vectors, each of which has a nonzero value only in the kth entry, defining the bias value and also identifying the kth sensor as biased. A vector with zeros in all entries is also included in the data set to account for the case where no bias is present. The bias values for each sensor are equally spaced, based on the noise standard deviation σ over a range of possible values. The minimum bias value is defined by the detection threshold while the maximum value is set in accordance with a bound that would typically disqualify the sensor for being out of range, as shown in Fig. 4. The detection threshold is set large enough so that noise is unlikely to be interpreted as a bias. In this paper, the threshold is set to 4σ while the upper bound is set to 20σ. Again, σ value indicates the standard deviation of steady-state noise.

At steady-state conditions, the control system employed in the current study maintains a certain sensor output at a target value. When this regulated sensor output is biased, the control system adjusts actuator commands to match the biased sensor output with the target, causing other nonregulated sensor outputs to shift from their baseline values. Therefore, a bias in the regulated sensor output causes shifts in multiple sensors, and a bias vector that contains only one nonzero value cannot cancel out such influence of this particular biased sensor. To overcome this problem, bias vectors with more than one non-zero value are needed in the case of the regulated sensor output being biased. These nonzero values in a bias vector can be determined using the engine model through the following steps: 1) inject a bias with a certain magnitude to the regulated sensor and then 2) determine the corresponding shift in the nonregulated sensor outputs. By repeating the steps 1 and 2 for different bias magnitudes, a new set of bias vectors can be constructed for the case of the regulated sensor output being biased. In this paper, however, these steps are not taken; the regulated sensor is not included in the sensor list of the Engine Model Section, assuming that this sensor will not be biased.

Neural-Network Estimator Design

The neural-network estimator is the key element of the hybrid estimator. As mentioned earlier, the neural-network estimator does not need to account for sensor bias, but it still has to tolerate the effects of measurement uncertainty as a result of steady-state noise. The robustness of the estimator can be improved by using noise-corrupted sensor measurements during training so that the neural networks will learn to distinguish the range of measurement shifts caused by noise and those caused by health degradation. However, because the number of health degradation scenarios that an engine can encounter is virtually infinite, it is still a challenging problem to develop an estimator that performs adequately well.

During a preliminary study of the neural-network estimator development, it was found that sensor measurements from at least two operating points were needed in order to achieve the desired estimation performance level. The difficulty in estimating health parameters can be caused by sensor location, sensor noise, highly nonlinear engine behavior, or a combination of these. Table 1 compares the performance of two estimators: one designed using simulated data from cruise condition and another designed using simulated data from cruise and takeoff conditions. For the two-point design, takeoff was selected as the second operating point because of the limitations of the range that the current engine model can be operated. Both designs are composed from nine multiple-input, single-output subestimators, each of which was developed using a feed-forward neural network. The neural-network estimators were trained by backpropagation using about 3000 degraded engines. The single-point design has 12 inputs with one hidden layer of 30 neurons (12-30-1) while the two-point design has 24 inputs with one hidden layer of 40 neurons (24-40-1). The table shows the standard deviation and mean value of estimation errors. The result was obtained using the sensor measurements of 500 degraded engines without noise. These 500 engines were not used in the neural-network training. Although a single-point diagnostic approach is desired for practical reasons discussed earlier, it was found to provide unsatisfactory estimation accuracy. Thus a multipoint estimator is utilized. Some of the health parameters are more difficult to accurately estimate than others.

Genetic-Algorithm Optimization Process

To find an optimal solution in the bias data set, the GA search sequence shown in Fig. 3 proceeds as follows. First, a bias vector $\hat{\boldsymbol{b}}_i$ selected from the bias data set is subtracted from physical sensor measurement deltas (deviations from the baseline) $\Delta\boldsymbol{y}$, and the resultant vector is fed into the neural-network estimator. If the selected bias vector is identical or close to the true bias $\boldsymbol{b}$, then the bias in the measurements is cancelled out. This allows the neural-network estimator to generate an accurate estimation of the health parameter vector $\hat{\boldsymbol{p}}_i$ from the bias-free measurements. The engine model is run with inputs of $\hat{\boldsymbol{b}}_i$ and $\hat{\boldsymbol{p}}_i$ to synthesize engine sensor outputs $\hat{\boldsymbol{y}}_i$ for comparison with the physical sensor measurements.

For each selected bias vector $\hat{\boldsymbol{b}}_i$, the following cost function, which accounts for the multipoint estimation, is computed:

$$J_i = \left\{ \sum_{j=1}^{m} \left[\frac{(\hat{y}_i)_j - y_j}{W_j} \right]^2 \Bigg|_{\text{Cruise}} + \sum_{j=1}^{m} \left[\frac{(\hat{y}_i)_j - y_j}{W_j} \right]^2 \Bigg|_{\text{Takeoff}} \right\}^{\frac{1}{2}} \tag{3}$$

where m is the number of sensors and

$$W_j = \begin{cases} \sigma_j & \text{when} \quad j = k \\ 3\sigma_j & \text{otherwise} \end{cases} \tag{4}$$

where σ_j is a standard deviation of noise in sensor j and k is the index of the nonzero entry of a selected bias vector. The parameter W_j normalizes the estimation error while imposing a larger penalty for discrepancies in the kth sensor. If a selected bias vector contains a bias estimation value in the wrong sensor, the estimation error in the kth entry is magnified. In the current problem setup, the noise standard deviation for the sensors varies with operating point. Therefore, in the preceding equation W_j and noise contained in y_j are based on the corresponding sensor σ values at the specific operating point. The bias value, on the other hand, is set to a constant number; it does not vary with operating point. The bias values in the bias data set and the actual bias value used in the later examples are based on the σ value at the cruise condition.

A value indicating the estimation accuracy, or fitness value, for each selected bias vector is defined as

$$\text{Fitness}_i = K / J_i \tag{5}$$

where K is a constant for normalization. The K value was selected so that fitness value larger than 1.0 indicates good agreement between model outputs and physical sensor measurements. The fitness value becomes larger as the output error between $\hat{\boldsymbol{y}}_i$ and y diminishes.

A unique aspect of the GA search process is that a set of multiple points in the solution space is evaluated at each iteration, and the content of this set is updated from iteration to iteration. In the GA problem setup, each bias vector in the data set is referred to as an "individual," and a number of individuals are selected from the data set to construct a "population." At each iteration, or "generation," the entire population is evaluated, and a fitness value is assigned to each individual. The higher the fitness value, the higher the probability that the corresponding individual will survive into the next generation. The population of the next generation is constructed from individuals of the previous generation and individuals newly introduced from the data set. As the population is updated from generation to generation, those individuals with high fitness values will occupy the major portion of the population. The objective of the GA optimization is to find the best individual among the data set through this search process. Unlike gradient search methods, the GA search process is initialized with multiple evaluation points in the solution space; this helps to avoid convergence to a local peak in the highly nonlinear environment. Moreover, the fitness values indicate the level of confidence in the estimation. If an appropriate individual does not exist in the solution space, the fitness values of searched individuals will remain small. In such a case, the best individual should not be relied upon for accurate diagnosis of engine health although an anomalous condition can exist.

The GA search process is generally run for many generations until the set of individuals constructing the population converges to a single individual. In the current study, the GA is run for relatively few generations. In this highly nonlinear and noisy environment, it is possible to have dissimilar degradation scenarios producing similar sensor signatures, as was illustrated in Fig. 2. Running the GA until convergence to a single individual can lead to erroneous conclusions regarding engine health. After the search process, the searched bias vectors are ranked based on their corresponding fitness values. A list of several fault candidates can help to avoid false alarms or missed detections. Moreover, running the GA for fewer generations can save a significant amount of computing time.

Performance Evaluation of Hybrid Estimator

This section shows some of the results obtained from an extensive assessment of the hybrid estimator. Tables 2 and 3 show the performance of the hybrid estimator for a health degradation case where sensor measurements contain no bais. The set of actual health parameters shown in Table 2 was not a part of the neural-network estimator training set. There are no clear guidelines to define the adequate performance level in the highly nonlinear environment of the current study. In this paper, the performance of the estimator is considered satisfactory if the maximum health estimation error is less than 30%. Tables 2 and 3 show both good sensor matching and good health estimation accuracy, meeting with the performance requirements. Estimation accuracy is influenced by sensor noise.

When one of the sensors is biased, the neural-network estimator alone can no longer accurately estimate health parameters. The following example shows a case where the fuel flow sensor has a 9.5σ bias with the same health degradation as shown in Table 2. This bias magnitude is in the medium range of the current problem setup. After the GA search process, the hybrid estimator provides the rank of bias estimations as shown in Table 4 and the corresponding plots shown in Fig. 5. Table 4 shows the identification numbers of biased sensors, bias values, and corresponding fitness values. Sensor matching is considered adequate if the fitness value is larger than 0.75 and is considered very good if the fitness value is larger than 1. Therefore, the top four bias estimations are good candidates for representing the actual bias. Figure 5 shows the fitness values

Table 3 Estimation performance without sensor bias: sensor estimation

	Normalized estimation error $(\hat{y} - y)/3\sigma$	
Sensor	Cruise	Takeoff
N2	0.750	−0.069
N25	−0.155	0.755
T27	−0.378	0.007
T3	0.482	0.028
PS15	0.146	0.029
PS21	−0.059	0.163
P27D	0.281	0.600
PS3	0.155	1.095
P42	−0.235	0.467
WF36	−0.222	0.412
A8	0.198	0.121
A16	−0.263	−0.062

Table 2 Estimation performance without sensor bias: health parameter estimation

Health parameter	Actual condition, %	Estimated condition, %	% Error $(\hat{p} - p)/p * 100$
FAN efficiency	−2.900	−2.793	−3.682
FAN flow	−1.800	−1.819	1.029
BST flow	0.000	0.000	——
HPC efficiency	−2.300	−2.177	−5.367
HPC flow	−1.900	−2.016	6.078
HPT efficiency	−1.400	−1.612	15.138
HPT flow	1.000	0.883	−11.750
LPT efficiency	−2.000	−2.199	9.930
LPT flow	2.100	2.093	−0.320

of individuals (bias vectors) selected by the GA during the search process. The horizontal axis varies from -20σ to 20σ with a 1σ increment. The bias vector representing the no-bias case is shown at the center of all plots, providing a baseline for comparison between estimations with and without bias detection. As mentioned earlier, the detection threshold is set to 4σ. The bias data set contains 409 individuals, and the population size is set to 50. The initial population included four individuals from each sensor, two individuals for each bias direction.

Tables 5 and 6 shows the estimation performance with and without sensor bias detection logic. The estimation result of the individual ranked first in Table 4 is shown. For the estimator with bias detection logic (neural network with GA), the performance requirement is met. Although the estimation errors of HPT efficiency and HPT flow coefficient are relatively high among the health parameters, a similar trend was noticed in the preceding example where no bias was present, as was shown in Table 2. When the health parameters are estimated without bias detection logic (neural network without GA), the neural-network estimator attributes the sensor bias to health parameters, resulting in poor health parameter and sensor estimation performance. This comparison illustrates the highly effective performance of the hybrid estimator in isolating a sensor bias while maintaining a high level of health parameter estimation accurately.

The task of bias detection and estimation is easier for larger biases. With a large bias in the measurements, the cost function value of Eq. (3) ideally remains large unless the bias is canceled out by an accurate estimate. This task becomes more difficult for small biases that are less distinguishable from noise. Table 7, Fig. 6, and Tables 8 and 9 show a case where the fuel flow sensor has a 4.5σ bias with the same health degradation as shown in Table 2. Table 7 and Fig. 6 show that the individuals representing the bias in the correct sensor (WF36) no longer dominate the GA population as they did in the preceding case with a larger bias value. Depending on the sensor noise profile, this ranking can change, and the correct sensor might not be ranked highest. The performance goal of the hybrid estimator is to at least capture the correct sensor in the ranking of plausible solutions in order to avoid missed detection. For smaller bias magnitudes, the robustness of the neural-network estimator is demonstrated. The bias vector representing the no-bias case (Sensor ID 0) is ranked fourth overall, and the corresponding health estimation and sensor matching shown in Tables 8 and 9 are well within the acceptable range.

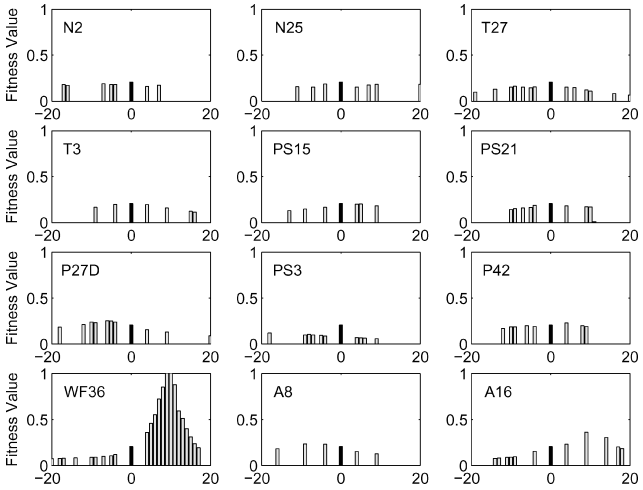

Fig. 5 Fitness values of individuals selected by GA search (case 1: 9.5σ bias in WF36).

Table 4 Rank of sensor bias estimation after GA search (case 1: 9.5σ bias in WF36)

Rank	Sensor ID	Bias (σ)	Fitness
1	10 (WF36)	10	1.036
2	10 (WF36)	9	1.020
3	10 (WF36)	11	0.878
4	10 (WF36)	8	0.852
5	10 (WF36)	7	0.723
6	10 (WF36)	12	0.594
7	10 (WF36)	6	0.554
8	10 (WF36)	13	0.512
9	10 (WF36)	5	0.458
10	10 (WF36)	14	0.402

Table 6 Estimation performance with and without bias detection logic (case 1: 9.5σ bias in WF36): sensor estimation

		With bias detection			Without bias detection	
			Error $(\hat{y}-y)/3\sigma$		Error $(\hat{y}-y)/3\sigma$	
Sensor	Actual bias	Estimated bias	Cruise	Takeoff	Cruise	Takeoff
N2	0	0	0.751	−0.070	3.432	−0.109
N25	0	0	−0.154	0.754	−1.896	−0.352
T27	0	0	−0.377	0.006	0.453	0.078
T3	0	0	0.482	0.027	0.204	−0.275
PS15	0	0	0.146	0.030	−1.439	−0.369
PS21	0	0	−0.058	0.163	0.767	0.100
P27D	0	0	0.281	0.600	1.217	0.543
PS3	0	0	0.157	1.091	−3.064	−10.008
P42	0	0	−0.234	0.466	−0.561	0.194
WF36	9.5σ	10σ	−0.055	0.490	−2.906	−0.645
A8	0	0	0.198	0.120	2.313	0.397
A16	0	0	−0.263	−0.063	0.159	−0.488

Table 7 Rank of sensor bias estimation for small bias (case 2: 4.5σ bias in WF36)

Rank	Sensor ID	Bias (σ)	Fitness
1	10 (WF36)	5	1.035
2	10 (WF36)	4	1.022
3	10 (WF36)	6	0.878
4	0 (No bias)	0	0.863
5	9 (P42)	4	0.828
6	12 (A16)	4	0.813
7	12 (A16)	5	0.776
8	11 (A8)	−4	0.776
9	9 (P42)	5	0.765
10	12 (A16)	6	0.757

Table 5 Estimation performance with and without bias detection logic (case 1: 9.5σ bias in WF36): health parameter estimation

		With bias detection		Without bias detection	
Health parameter	Actual condition, %	Estimated condition, %	% Error	Estimated condition, %	% Error
FAN efficiency	−2.900	−2.788	−3.876	−2.950	1.722
FAN flow	−1.800	−1.811	0.596	−1.819	1.076
BST flow	0.000	0.000	——	−0.134	——
HPC efficiency	−2.300	−2.172	−5.578	−2.305	0.234
HPC flow	−1.900	−2.027	6.658	−1.497	−21.213
HPT efficiency	−1.400	−1.614	15.254	−1.715	22.516
HPT flow	1.000	0.875	−12.484	2.201	120.045
LPT efficiency	−2.000	−2.197	9.857	−2.303	15.146
LPT flow	2.100	2.083	−0.819	2.393	13.942

Table 8 Estimation performance with and without bias detection logic (case 2: 4.5σ bias in WF36): health parameter estimation

		With bias detection		Without bias detection	
Health parameter	Actual condition, %	Estimated condition, %	% Error	Estimated condition, %	% Error
FAN efficiency	−2.900	−2.787	−3.887	−2.865	−1.224
FAN flow	−1.800	−1.810	0.538	−1.864	3.557
BST flow	0.000	0.000	——	0.000	——
HPC efficiency	−2.300	−2.175	−5.456	−2.228	−3.137
HPC flow	−1.900	−2.026	6.624	−1.881	−1.018
HPT efficiency	−1.400	−1.608	14.876	−1.642	17.259
HPT flow	1.000	0.877	−12.310	1.235	23.506
LPT efficiency	−2.000	−2.197	9.824	−2.227	11.330
LPT flow	2.100	2.085	−0.706	2.220	5.723

Table 9 Estimation performance with and without bias detection logic (case 2: 4.5σ bias in WF36): sensor estimation

			With bias detection		Without bias detection	
			Error $(\hat{y}-y)/3\sigma$		Error $(\hat{y}-y)/3\sigma$	
Sensor	Actual bias	Estimated bias	Cruise	Takeoff	Cruise	Takeoff
N2	0	0	0.759	−0.070	1.237	−0.021
N25	0	0	−0.149	0.754	−0.365	0.674
T27	0	0	−0.376	0.006	−0.256	−0.002
T3	0	0	0.483	0.027	0.409	−0.044
PS15	0	0	0.144	0.029	−0.075	0.057
PS21	0	0	−0.057	0.162	−0.014	−0.115
P27D	0	0	0.283	0.600	0.316	0.278
PS3	0	0	0.161	1.093	−0.593	−1.506
P42	0	0	−0.232	0.466	−0.362	0.260
WF36	4.5σ	5σ	−0.052	0.489	−1.617	−0.198
A8	0	0	0.203	0.120	0.497	0.117
A16	0	0	−0.260	−0.063	−0.269	−0.201

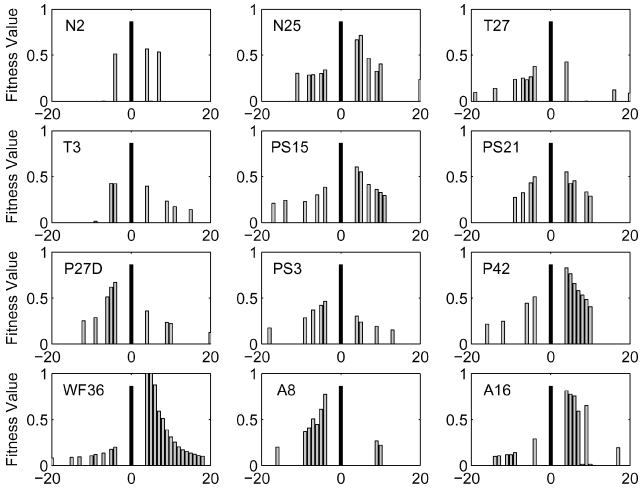

Fig. 6 Fitness values of individuals selected by GA search (case 2: 4.5σ bias in WF36).

Remarks on Hybrid Approach

Because of the high complexity of aircraft gas turbine engines, their associated diagnostic systems must possess the capability to handle multiple tasks. In this paper, for instance, the sensor output validation task was carried out along with the component performance monitoring task in order to avoid false alarms. In such a multitasking problem setting, utilization of multiple diagnostic techniques in an integrated manner can be an effective way to obtain successful results. Another example of a hybrid approach can be found in Ref. 14, where autoassociative neural networks (AANN) and GA were integrated for sensor fault diagnostics in the presence of a single component fault. In this reference paper, the task of sensor noise filtering while retaining anomalous sensor signature caused by a component fault was handled by a noise-filtering AANN, whereas the sensor bias detection and accommodation task was handled by the combination of a self-mapping AANN and GA. Although the objectives of the current and reference papers are different, integration of multiple diagnostic techniques was successfully demonstrated as an effective approach to meet the diagnostic objectives.

Discussion

The concept of integrating neural networks and GA for steady-state trend monitoring of aircraft gas turbine engines was presented in this paper. The hybrid estimation technique exhibited excellent performance; however, design refinement must be made for further improvement. In this section, some issues that need to be addressed to make this technique applicable to real systems are discussed.

First, the influence of neural-network and GA design parameters on overall performance must be investigated. The neural-network estimators developed in this paper have one hidden layer of a specific number of neurons. Different structures of hidden layers or different numbers of neurons can improve the accuracy of health parameter estimation. In the GA optimization process, parameters such as crossover and mutation probabilities influence the effectiveness of the search process. In this paper, 50% crossover and 30% mutation probabilities were used. Better performance can be obtained by adjusting these numbers.

A particular sensor that is regulated by the control system during steady-state conditions was not included in the sensor suite used in this study. Because the regulated sensor output can be biased as well as other sensors, this sensor must be monitored for bias detection. As discussed earlier, the bias vectors that are needed to cancel out the influences of bias in this particular sensor can be constructed using the engine model. These bias vectors must be added to the bias data set, and then the hybrid estimator must be reevaluated.

The cost function of the GA optimization used the snapshot data of one flight in a discrete manner. In other words, the cost function is based only on the knowledge obtained from a certain flight. Because it is known that component degradation progresses gradually with time, the past trend of health parameters can be incorporated into the cost function. For instance, it can be expected that the health condition at the current time frame has small deviations from the estimated condition at the preceding time frame. Based on this knowledge, differences in the health parameter estimates between the current and the past time frames can be included in the cost function in addition to sensor matching terms in Eq. (3). This modification will restrict the current estimates to be within some range from the previous estimates, and such a restriction might help to reduce the adverse effect that appeared as the nonunique relationship between the health degradation and the sensor measurement shifts.

Although it was assumed that one sensor might be biased at a time, the structure of the hybrid estimator can be expanded to account for multiple sensor biases through a sequential or simultaneous search. A sequential search could be done by continuing the GA search process after a single biased sensor is detected. A simultaneous search could be done by adding bias vectors that have multiple nonzero values to the bias data set. It should be understood, however, that the complexity of the diagnostic problem and the difficulty in

obtaining reliable diagnostic results will increase as the number of biased sensors increases.

Conclusions

A hybrid estimation technique for aircraft engine performance diagnostics was presented in this paper. The hybrid architecture consists of neural networks and genetic algorithms, which function synergistically for estimating health parameters from sensor outputs even in the presence of a biased sensor. Neural networks are well suited for estimating health parameters in a highly nonlinear environment. However, a major problem arises when the size of training data set becomes prohibitively large. To avoid this problem while improving the robustness to measurement uncertainty, genetic algorithms were applied for sensor bias detection. The hybrid estimator exhibited excellent performance when at most one sensor was biased. The task of health parameter estimation became more difficult when the bias was of smaller magnitude and was thus less distinguishable from the standard noise level. Because measurement shifts as a result of health degradation are often small compared to sensor noise, and distinctive health degradation cases do not necessarily result in distinctive measurement shifts, it is difficult to obtain one solution with a high level of confidence. This problem was handled by ranking several potential solutions for a given set of anomalous sensor measurements. This approach reveals a potential method of reducing false alarms and missed detections.

There are, however, areas for further improvement. A systematic way of selecting and/or locating sensors for health estimation is desired. Simply increasing the number of sensors for health diagnostics does not guarantee improved estimation performance. Moreover, as the number of sensors increases, the chance of having biases in multiple measurements increases. Another desired improvement is a reduction of the required computing time. A real-time, onboard diagnostic system that can be integrated with a control system is desirable, but such a system is difficult to develop with the proposed architecture. Alternative approaches that allow improved computing speed without sacrificing reliability must be investigated for the development of a comprehensive health management system.

References

[1]Simon, D. L., "An Overview of the NASA Aviation Safety Program Propulsion Health Monitoring Element," AIAA Paper 2000-3624, July 2000.

[2]Urban, L. A., "Gas Path Analysis Applied to Turbine Engine Condition Monitoring," AIAA Paper 72-1082, Nov. 1972.

[3]Volponi, A. J., "Sensor Error Compensation in Engine Performance Diagnostics," American Society of Mechanical Engineers, Paper 94-GT-58, June 1994.

[4]Doel, D. L., "TEMPER—A Gas Path Analysis Tool for Commercial Jet Engines," *Journal of Engineering for Gas Turbines and Power*, Vol. 116, No. 1, Jan. 1994, pp. 82–89.

[5]Doel, D. L., "An Assessment of Weighted-Least-Squares-Based Gas Path Analysis," *Journal of Engineering for Gas Turbines and Power*, Vol. 116, No. 2, April 1994, pp. 366–373.

[6]Kerr, L. J., Nemec, T. S., and Gallops, G. W., "Real-Time Estimation of Gas Turbine Engine Damage Using a Control Based Kalman Filter Algorithm," American Society of Mechanical Engineers, Paper 91-GT-216, June 1991.

[7]Luppold, R. H., Roman, J. R., Gallops, G. W., and Kerr, L. J., "Estimating In-Flight Engine Performance Variations Using Kalman Filter Concepts," AIAA Paper 89-2584, July 1989.

[8]Zedda, M., and Singh, R., "Fault Diagnosis of a Turbofan Engine Using Neural Networks: A Quantitative Approach," AIAA Paper 98-3602, July 1998.

[9]Zedda, M., and Singh, R., "Gas Turbine Engine and Sensor Fault Diagnosis Using Optimisation Techniques," AIAA Paper 99-2530, June 1999.

[10]Gulati, A., Zedda, M., and Singh, R., "Gas Turbine Engine and Sensor Multiple Operating Point Analysis Using Optimization Techniques," AIAA Paper 2000-3716, July 2000.

[11]Adibhatla, S., and Lewis, T. J., "Model-Based Intelligent Digital Engine Control (MoBIDEC)," AIAA Paper 97-3192, July 1997.

[12]DePold, H. R., and Gass, F. D., "The Application of Expert Systems and Neural Networks to Gas Turbine Prognostics and Diagnostics," *Journal of Engineering for Gas Turbines and Power*, Vol. 121, No. 4, 1999, pp. 607–612.

[13]Stamatis, A., Mathioudakis, K., Berios, G., and Papailiou, K., "Jet Engine Fault Detection with Discrete Operating Points Gas Path Analysis," *Journal of Propulsion and Power*, Vol. 7, No. 6, 1991, pp. 1043–1048.

[14]Lu, P.-J., and Hsu, T.-C., "Application of Autoassociative Neural Network on Gas-Path Sensor Data Validation," *Journal of Propulsion and Power*, Vol. 18, No. 4, 2002, pp. 879–888.